

# INTERNATIONAL SOCIETY FOR SOIL MECHANICS AND GEOTECHNICAL ENGINEERING



*This paper was downloaded from the Online Library of the International Society for Soil Mechanics and Geotechnical Engineering (ISSMGE). The library is available here:*

<https://www.issmge.org/publications/online-library>

*This is an open-access database that archives thousands of papers published under the Auspices of the ISSMGE and maintained by the Innovation and Development Committee of ISSMGE.*

# Ice gouging analysis using NorSand critical state soil model

Farzad Eskandari

*Faculty of Engineering, Memorial University of Newfoundland, St. Johns, Canada*

Ryan Phillips

*C-CORE, Memorial University of Newfoundland, St. Johns, NL, Canada*

Bipul Hawlader

*Faculty of Engineering, Memorial University of Newfoundland, St. Johns, NL, Canada*



## ABSTRACT

In the arctic and other cold regions, subsea pipelines are exposed to various hazards such as pressure ridges or icebergs gouging the seabed which can impose distress to the pipe due to seabed deformation. Understanding the pipe response provides the basis to determine a safe burial depth in which the seabed gouges would not jeopardize the integrity of the pipeline while it is reasonable cost-wise. Numerical analysis is proven to be a reliable tool to capture the seabed behaviour during the ice gouging event and simulate the subgouge deformations. Most of the soil constitutive models available in commercial finite element (FE) packages do not appropriately simulate the dilative behaviour of soil. NorSand critical state soil model improved the simulation of behaviours of sand for various loading conditions. In this paper NorSand model is implemented in ABAQUS Explicit user subroutine VUMAT and calibrated against drained triaxial test data. A 3D finite element model is developed in ABAQUS Explicit to simulate the ice gouging events in the sandy subsea.

## RÉSUMÉ

Dans les régions arctiques et autres régions froides, les pipelines sous-marins sont exposés à divers risques tels que les crêtes de pression ou par le raclement des fonds marins par les icebergs qui peuvent imposer des contraintes mécaniques aux tuyaux en raison de la déformation du fond marin. Comprendre la réponse du tuyau fournit la base pour déterminer une profondeur d'enfouissement sécuritaire à laquelle les raclements des fonds marins ne compromettrait pas l'intégrité du pipeline et ce avec des coûts raisonnables. L'analyse numérique est avérée être un outil fiable pour saisir les fonds marins comportement pendant les gougeage de la glace et de simuler les déformations en dessous des raclements. La plupart des modèles constitutifs du sol disponible en élément commercial finis ne simule pas correctement le comportement de dilatation du sol. Le modèle critique de l'état du sol NorSand améliore la simulation des comportements de sable sous différentes conditions. Dans cet article NorSand modèle est implémenté dans ABAQUS Explicit utilisateur VUMAT sous-routine et étalonné par rapport aux données d'essai de drainages triaxial. Un modèle tridimensionnel par éléments finis est développé dans ABAQUS Explicit pour le gougeage de glace dans le sous-sol sableux.

## 1 INTRODUCTION

Floating ice masses are directed into shallow water under wind and current action. These masses could cause deep gouges into seabed when they ground in shallow waters. For instance in the Beaufort Sea and the Arctic Islands the gouging occurs from shore to the waters as deep as 50 meters. Although some extreme gouge depths have been measured in excess of 5 meters, average gouge depths are typically smaller in magnitude and are a function of water depth and soil type. Surveys show that deeper ice gouges happen in deeper waters such as Davis Strait in Labrador Sea and the Grand Banks in southeast coast of Newfoundland.

In the Arctic, ice gouging is the main threat to the offshore pipelines. Ice gouging phenomenon is a soil-structure interaction problem which consists of three parts: ice, soil and pipeline. The pipeline system reinforces the surrounding soil locally therefore the coupled response of pipe/seabed should be considered under ice gouging.

The ice gouging process starts with the contact of the ice and soil. Initially the ice can simultaneously both penetrate and advance horizontally in the soil but ultimately it reaches a steady state situation where there is no more penetration and the ice gouges the seabed at near constant depth. Investigations have shown that even deep gouges are being formed at present. As the result ice gouging has to be considered one of the active hazards that may jeopardize the integrity of the offshore pipelines in the energy industry and therefore it should be carefully addressed.

The mechanism of ice gouging can be studied through three different methods using field gouge tracks, laboratory scale tests and numerical models. Numerical simulation is a popular method in the study of ice gouging. It has the advantage of being able to simulate the gouging response under different boundary conditions and loading cases or soil materials. The selection of an appropriate constitutive model to define the materials that are involved in a problem is essential for an accurate numerical analysis. These models should be able to account for

different stress paths. They also should be simple in terms of providing the input parameters with number of common physical tests. In addition it is important that they are based on the realistic interpretations of material stress-strain behaviour of the ice gouging event. Kenny et al. (2005) showed the finite element analysis can simulate key aspects of ice/seabed/pipe interaction adequately.

Existing soil constitutive models are relatively simplistic for use in finite element analyses based on single phase explicit formulation used with adaptive meshing. In order to study different aspects of drained ice gouging in the sand, Barrette and Phillips (2011) enhanced the built-in Drucker Prager model of ABAQUS by defining a Solution Dependent Variable in a subroutine to vary the dilation angle of the soil in accordance with the real behaviour and compared their results to gouge test data.

ABAQUS Explicit allows users to develop their own material models and enhance the explicit analyses by implementation of user defined material subroutine VUMAT. This feature in ABAQUS is helpful in problems like ice gouging where the available built-in models have a number of limitations. Figure 1 shows how the user subroutine VUMAT is incorporated in the ABAQUS Explicit analysis. An explicit analysis is divided into many small time increments. At the beginning of each time increment, based on the dynamic laws and equations of equilibrium the new configuration of the system is derived. The system deformation then accordingly is translated to strain increments. The current stress and user defined state variables as well as the strain increment are sent to the VUMAT subroutine. Subsequently based on the constitutive equations of any desired material model, the user material subroutine updates the stress components and state variables. The updated stress components and user defined state variables are eventually sent back to the ABAQUS Explicit solver and is utilized as VUMAT inputs in the next time step.

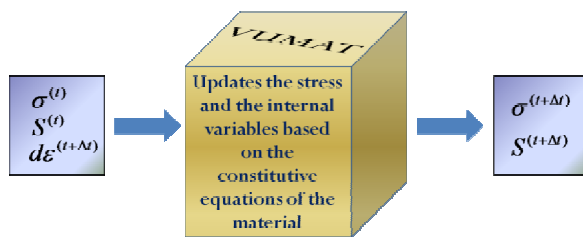


Figure 1. VUMAT in ABAQUS Explicit

Eskandari et al. (2010) developed a variant of Drucker-Prager Cap model using user material subroutine VUMAT to capture different responses of sands based on the initial density and stress level and to suppress the excessive dilation rate that the built-in Cap model yields.

NorSand has been reported to successfully capture the behaviour of sandy soils. In this study NorSand is implemented in an ABAQUS Explicit user subroutine to simulate the ice gouging event in the sand.

## 2 NORSAND A CRITICAL STATE MODEL

Sand behaviour is a function of initial conditions or more precisely initial void ratio,  $e$  and initial mean effective pressure,  $\sigma'_m$ . The results obtained from the laboratory tests have shown that the initial parameters of  $e$  and  $\sigma'_m$  do not determine the behaviour of sandy samples decisively if used separately and it is the combined effect of both of these two parameters that influences the soil behaviour and establishes the initial state. It is widely accepted that the behaviour of sands should be represented in term of a state parameter that combines the effects of void ratio and stress level together. The coupled effects of density and confining pressure on soil behaviour have been studied by a number of researchers (e.g. Roscoe and Poorooshasb 1963; Been and Jefferies 1985; Bolton 1986; Ishihara 1993; and Verdugo 1992). One common point in each of these studies is that an index was defined to describe the effects of initial state of sand on stress-strain behaviour. The index is a measure of the distance between initial state and ultimate state where the failure occurs. It has been shown that these indices better represent the soil state and stress-strain behaviour than the relative density ( $D_r$ ) which is generally used in geotechnical engineering (Cubrinovski and Ishihara 1998).

NorSand employs the same bullet like yield surface of Cam-Clay with the exception of applying an internal cap (Jefferies & Shuttle, 2005). The constitutive model NorSand is based on the critical state soil mechanics. The theory of critical state soil mechanics consists of two principles: 1) There exists a unique locus for critical state in the void ratio-stress space, and 2) the soils move toward the critical state as the shear strain evolves. The first principle suggests that in the  $q, p, e$  space a unique locus exist that in this region the soil can deform without any kind of restriction while the stress level and void ratio remain constant. This locus is called critical state line (CSL). The first principle defines the critical state and confirms its existence. The second principle can be interpreted such that the CSL portray the final position of all deforming processes of soils. The second principle could be expressed readily by choosing a simple criterion for deviation from critical state. This criterion is called the state parameter.

The state parameter which is defined as a function of void ratio and stress level should be measured according to a reference condition. Hence, it is required to determine an appropriate reference condition from a physical point of view. For the sake of simplicity and as an acceptable approximation it is possible to consider the critical state line in form of a unique and straight locus in  $e - \ln(p)$  and  $p - q$  spaces. By the term of unique it is intended to emphasize that the locus of this line is independent of test conditions such as sample preparation, drainage and strain rate.

The critical state is conventionally summarized in Equation 1.

$$\begin{aligned} q_c &= Mp_c \\ e_c &= \Gamma - \lambda_c \log p_c \end{aligned} \quad [1]$$

In Equation 1,  $M$  is the critical stress ratio,  $q_c$  is the critical deviator stress,  $p_c$  is the critical mean effective stress,  $\Gamma$  is the critical void ratio on the CSL that corresponds to a mean effective stress of 1 kPa and finally  $\lambda_c$  is the slope of CSL in the  $e - \ln(p)$  space.

Having the critical state line defined, Been and Jefferies (1985) represent the state parameter as the departure of current void ratio from that related to critical state at any time. This definition could be idealized mathematically as shown in Equation 2.

$$\psi = e - e_c \quad [2]$$

Physically positive values of state parameter represent that the soil is on wet side of the critical state that is just lightly overconsolidated. On the other hand a negative value of state parameter refers to a sample of soil on the dry side of critical state line in which soil is more highly overconsolidated.

Currently there are variant critical state models that are based on state parameter either explicitly or implicitly. From the most well-known examples of these models Manzari & Dafalias (1997), Wan & Guo (1998), Li et al. (1999) and Gajo & Wood (1999) could be named but the first critical state model that used state parameter was NorSand.

As an advantage, NorSand can represent the isotropic softening as well as isotropic hardening through its hardening law (Jefferies and Shuttle, 2002). The model defines a maximum limiting dilation based on the state parameter which as soon as the soil reaches this limit, the yield surface is free to shrink if required until the critical state is met.

NorSand uses eight model parameters which are described in Table 1.

Table 1. Input parameters of NorSand

Parameter	Description
$I_R$	Shear rigidity
$\nu$	Poisson's ratio
$\lambda$	Slope of critical state line
$\Gamma$	Critical state void ratio at mean effective stress of 1 kPa
$M_{tc}$	Critical stress ratio in triaxial compression condition
$\chi_{tc}$	Defines maximum dilatancy based on state parameter
$H$	Plastic hardening modulus
$\psi$	State parameter

### 3 MODEL VALIDATION

In order to validate the implementation of the critical state model NorSand in ABAQUS Explicit user subroutine a number of analyses are compared with triaxial laboratory tests as published by Jefferies and Been (2006). These analyses include three dense samples (D-1, D-2 and D-3) and three loose samples (L-1, L-2 and L-3) under drained condition. For the model parameters the same values that are suggested by Jefferies and Been (2006) are adopted. These parameters are summarized in Table 2

To perform these comparisons a 2D axisymmetric finite element model is created to simulate the triaxial condition. However, since the main objective of this implementation is to use NorSand for ice gouging simulation, which is a highly 3 dimensional problem, a 3 dimensional triaxial model is also created to examine the performance and validity of the user subroutine VUMAT in 3 dimensional space. The same set of input parameters were then used to compare the results of the 3D model with 2D axisymmetric model.

Table 2. Input parameters of the sample analysis as suggested by Jefferies and Been (2006)

	D-1	D-2	D-3	L-1	L-2	L-3
$I_R$	600	400	1000	150	250	400
$\nu$	0.33	0.33	0.33	0.33	0.33	0.33
$\lambda$	0.031	0.031	0.031	0.031	0.031	0.031
$\Gamma$	0.816	0.816	0.816	0.816	0.816	0.816
$M_{tc}$	1.26	1.26	1.26	1.18	1.18	1.18
$\chi_{tc}$	3.7	4	4.5	4	3.7	3.7
$H$	150	160	170	50	45	70
$\psi$	-0.08	-0.08	-0.08	0.070	0.045	0.040
$p_0$ (kPa)	140	300	60	1000	50	200

The three-dimensional finite element model for triaxial test is shown in Figure 2 illustrating uniform von Mises stress with less than 0.1% variation from 315 kPa.

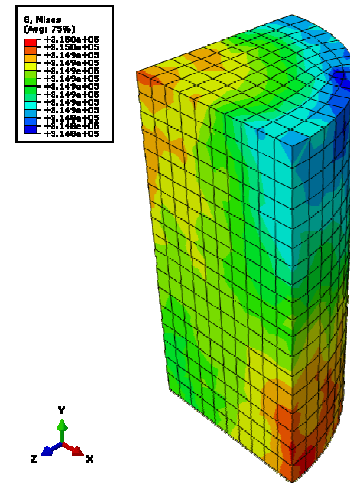


Figure 2. 3D Triaxial Model

Figure 3 to Figure 8 show the results of the analyses of dense samples under drained triaxial condition. On the other hand, in Figure 9 to Figure 14 the responses of loose samples of Erksak sand (Jefferies and Been 2006) are predicted using NorSand constitutive model.

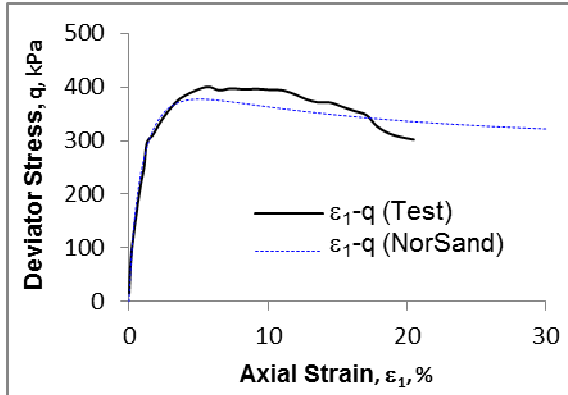


Figure 3. Test D-1, drained dense sand sample, deviatoric stress – axial strain

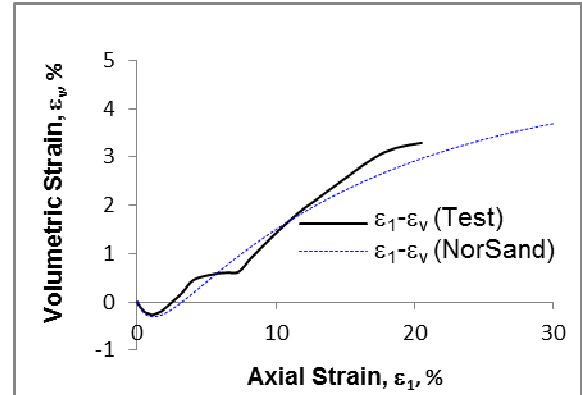


Figure 6. Test D-1, drained dense sand sample, volumetric strain – axial strain

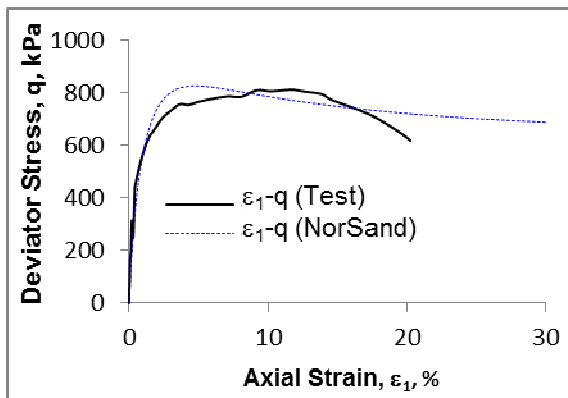


Figure 4. Test D-2, drained dense sand sample, deviatoric stress – axial strain

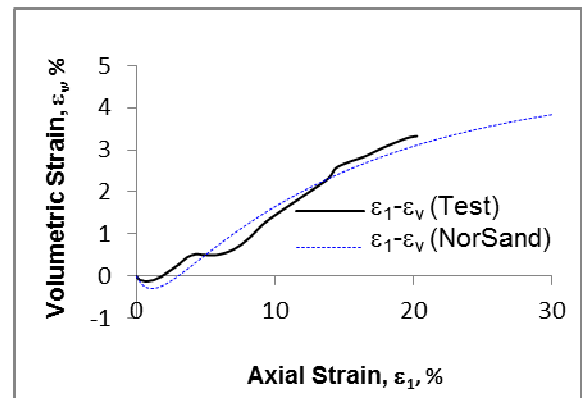


Figure 7. Test D-2, drained dense sand sample, volumetric strain – axial strain

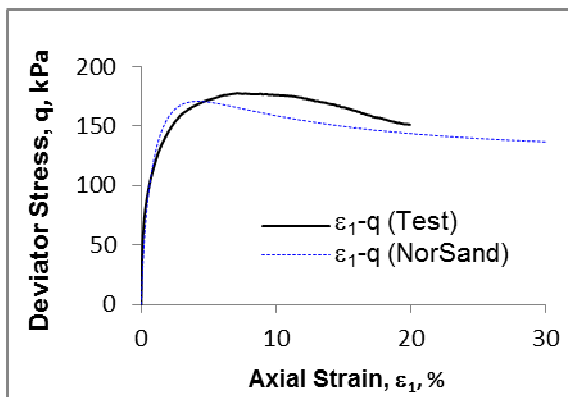


Figure 5. Test D-3, drained dense sand sample, deviatoric stress – axial strain

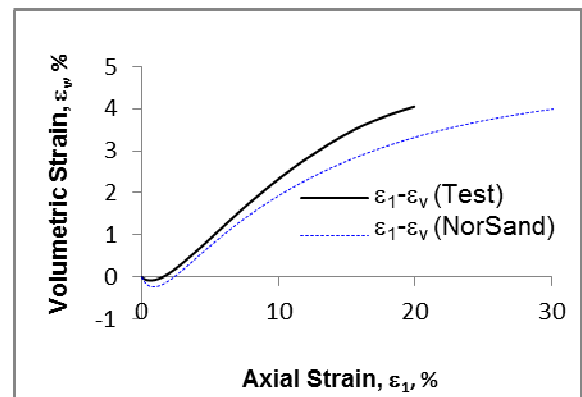


Figure 8. Test D-3, drained dense sand sample, volumetric strain – axial strain

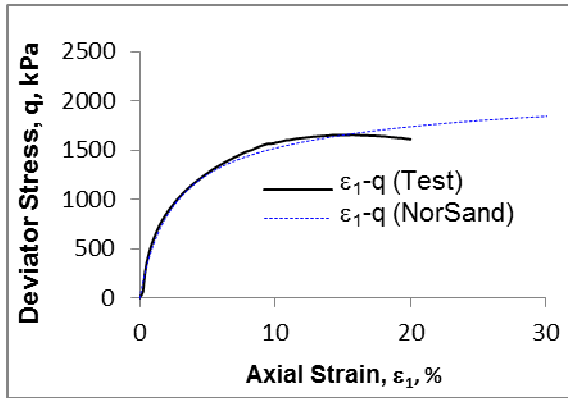


Figure 9. Test L-1, drained loose sand sample, deviatoric stress – axial strain

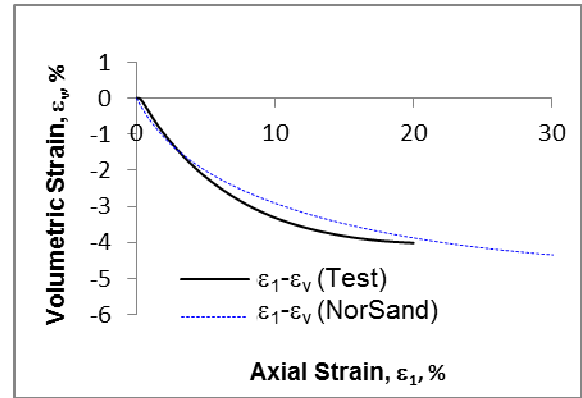


Figure 12. Test L-1, drained loose sand sample, volumetric strain – axial strain

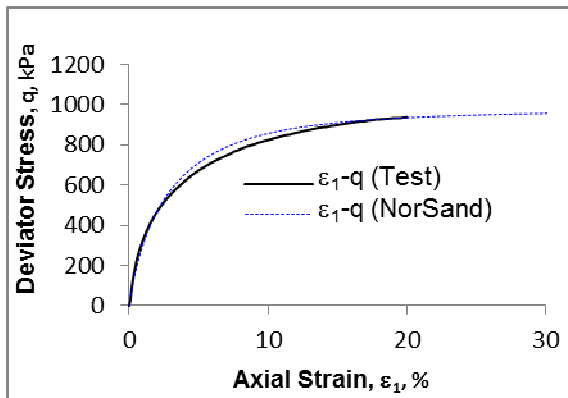


Figure 10. Test L-2, drained loose sand sample, deviatoric stress – axial strain

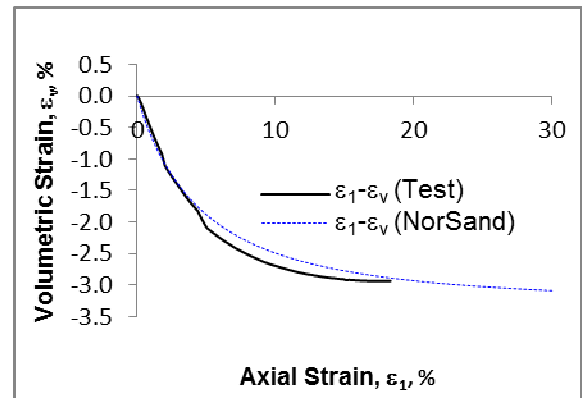


Figure 13. Test L-2, drained loose sand sample, volumetric strain – axial strain

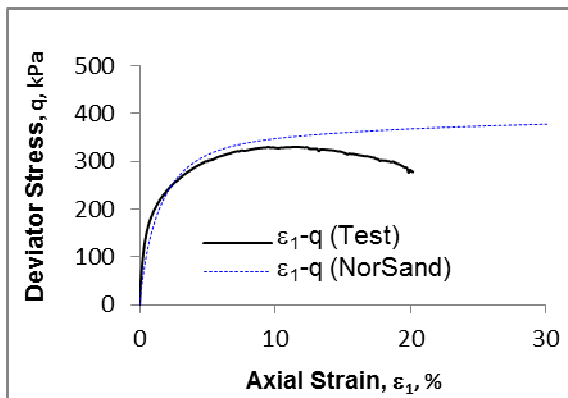


Figure 11. Test L-3, drained loose sand sample, deviatoric stress – axial strain

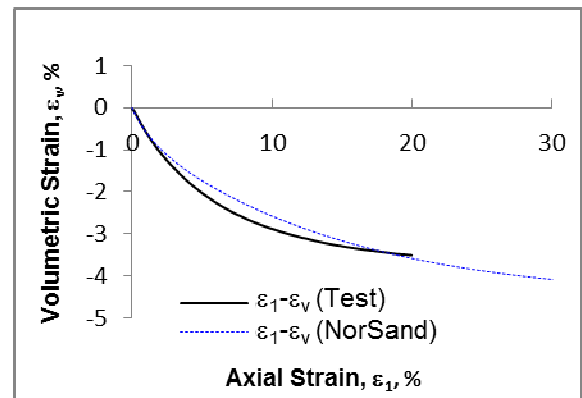


Figure 14. Test L-3, drained loose sand sample, volumetric strain – axial strain

All these comparisons show the predicted soil behaviour using NorSand implemented in ABAQUS Explicit is close to the published laboratory results.

Figure 15 shows that the results of the 3D model are identical to those of the 2D axisymmetric model. The stress and strain curves follow the same path in both 2D and 3D analyses. This indicates that the user subroutine works well in 3D condition as well and could be used in a general 3D problem like ice gouging. The input

parameters used in the analyses shown in Figure 15, are listed in Table 3. It should be noted that this 3D analysis is performed in triaxial condition. In reality the critical state ratio varies with Lode angle that influences the stress-strain behaviour (Bishop 1966). This phenomenon is captured in NorSand by defining the critical state ratio as a function of Lode angle. Therefore, in term of model formulation the only difference between general 3D analyses presented in Section 4 and a triaxial 3D analysis shown in Figure 15 is that in the latter the critical state ratio,  $M$ , does not change through the analysis.

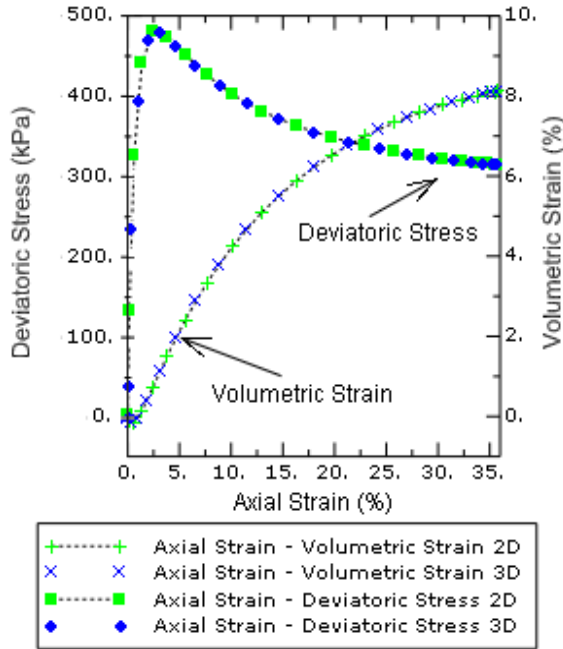


Figure 15. 3D Triaxial vs 2D axisymmetric triaxial results

Although it is not shown in Figure 15 the analyses results show that such a highly dense and dilative sample reaches to the critical state at about an axial strain of 50%.

Table 3. Input parameters for comparison of 3D and 2D model response

$I_R$	$\nu$	$\lambda$	$\Gamma$	$M_{tc}$	$\chi_{tc}$	$H$	$\psi$	$\rho_0$ (kPa)
600	0.33	0.031	0.816	1.3	3.8	300	-0.171	130

#### 4 THREE-DIMENSIONAL ICE GOUGING MODEL

To study the ice gouging problem a 3D model is created. The keel consists of rigid elements whereby the attack angle for the leading face is 30 degrees. The keel is idealized as a conical frustum with a diameter of 10 meters at the base. For the keel roughness a maximum shear stress of 150 kPa and a friction coefficient  $\mu$  of 0.2

is selected. Edges of the base are rounded to avoid numerical instabilities. In order to decrease the analysis time to reach the steady state of gouging the keel is initially indented into the soil. Figure 16 shows keel and soil in the model assembly.

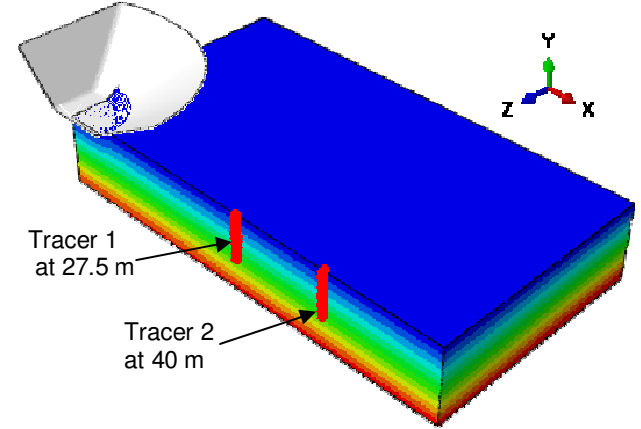


Figure 16. Keel and soil assembly in finite elements model

The keel advances horizontally at a model speed of 1 m/s gouging the seabed. The velocity of 1 m/s is suitable in this constitutive model as it is rate independent. In Figure 17 a typical seabed deformation caused by an ice gouging of 1 meter deep is shown. To avoid high mesh distortion under the large strains, the Arbitrary Lagrangian Eulerian (ALE) method is applied. The indented keel continues to move forward at the depth of 1 meter to a total of about 40 meters of horizontal displacement. The berm ahead of the advancing keel was not primed, so steady state gouge conditions were not attained in these preliminary analyses. In Figures 16 and 17 the soil dimensions are 55 m in X direction, 30 m in Z and 10 m in Y direction.

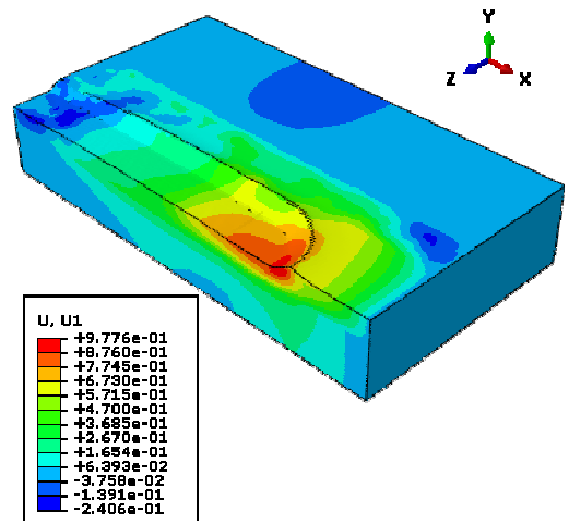


Figure 17. Horizontal soil deformation under ice gouging



The mesh dependency of the ice gouging model using the critical state model NorSand is initially investigated. In Figure 18 the keel reaction of two set of analyses is shown. Each set includes two different analyses which their input parameters are the same but mesh density of each analysis is different. Figure 18 shows that keel reaction for each set S1 and S2 scarcely depends on the number of the elements in the discretized domain. Table 4 lists the input parameters used for the analyses of set 1 and set 2. These analyses use the same input parameters except for state parameter  $\psi$  which is -0.05 in S1 and 0.1 in S2. In Table 5 the average elements size beneath the keel for each analysis shown in Figure 18 are presented. In this table the numbers shown in parentheses represent the total number of the elements in each model.

Table 4. Input parameters for comparison used in Figure 18 for mesh sensitivity

$I_R$	$\nu$	$\lambda$	$\Gamma$	$M_{lc}$	$\chi_{lc}$	$H$
50	0.452	0.031	0.816	1.5	3.7	70

Table 5. The average elements size<sup>1</sup> for mesh sensitivity analyses

S1 (217496)	S1 (335935)	S2 (339840)	S2 (279712)
30x25x35	27.5x16x30	25x12x25	25x15x27.5

<sup>1</sup> all sizes are in centimetre, element sizes are shown as length by depth by width where width refers to lateral direction

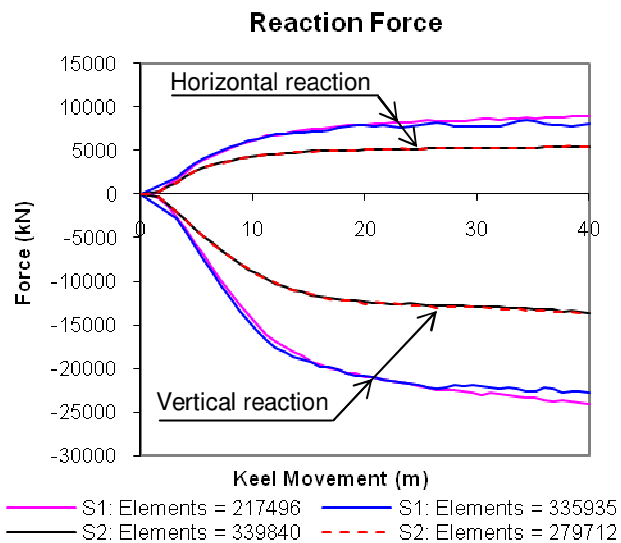


Figure 18. Mesh dependency in NorSand

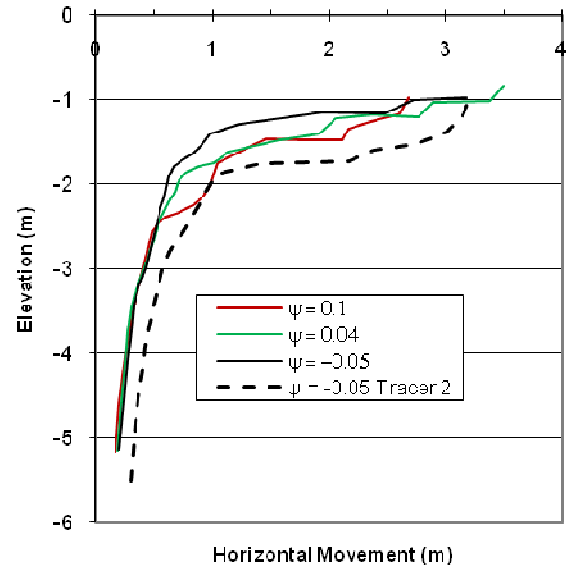


Figure 19. Subgouge deformation of the soil at tracer 1,  $M_{lc} = 1.4$ , other parameters as stated in Table 4

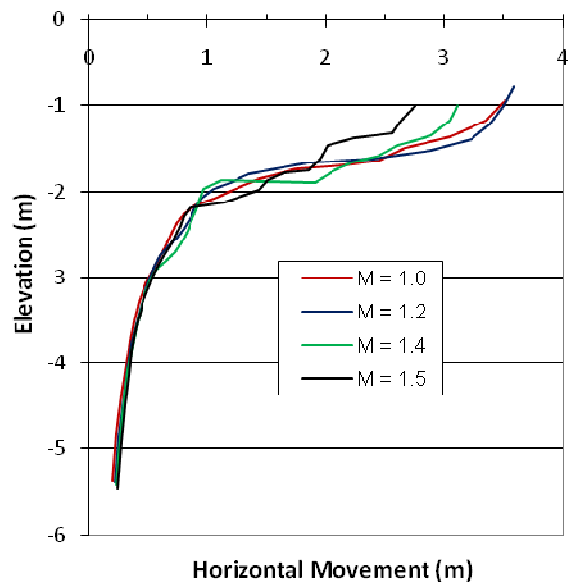


Figure 20. Subgouge deformation of the soil at tracer 2,  $\psi = 0.04$ , other parameters as stated in Table 4

Figure 19 and Figure 20 show the subgouge deformation at two different locations in the soil domain for a number of analyses. In these analyses some of the input parameters of the NorSand are changed to capture the gouging response on different soils. These subgouge profiles correspond to the soil deformation at the end of the analysis for each location. The first location, Tracer 1, is chosen at 27.5 m away from the beginning of the soil domain. The second location, Tracer 2, is at 40 meters away from the beginning of the soil domain. At the end of the analysis the keel has already passed Tracer 1 and is directly above the Tracer 2. The gouge base is at 1m depth. These deformations and associated reaction forces



are different to those of Barrett and Phillips (2011) due mainly to the difference in assumed keel roughness.

Figure 21 shows the response of vertical keel reaction after 40 m of keel displacement depending on the critical state ratio,  $M_{tc}$  and state parameter,  $\psi$ . The reactions increase with both soil strength and initial sand density.

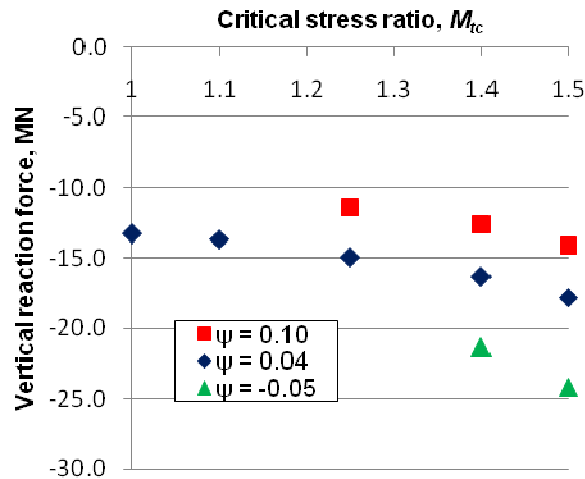


Figure 21. Variation of vertical force with critical state ratio,  $M_{tc}$  and state parameter,  $\psi$

## 5 CONCLUSION AND FUTURE WORK

NorSand plasticity model, developed on critical state framework, has shown better performance in modeling various laboratory test results of sand and has been used for a variety of geotechnical applications. In this research, the NorSand model has been used to simulate seabed response to ice gouging. ABAQUS finite element program has been used for numerical analysis. However, the NorSand model is not a built-in constitutive model in ABAQUS and therefore this model has been implemented in ABAQUS Explicit using user defined subroutine VUMAT.

Preliminary analyses show that the NorSand model is capable of predicting ice gouging behaviour. However, further study is required to calibrate the model performance, which is in progress.

In this study using the volume constraint method, the critical state model of NorSand was also extended to simulate the undrained behaviour of soils. In this method bulk modulus of water is chosen considerably larger than the bulk modulus of soil. This ensures the total soil volume change is insignificant as expected in undrained analyses. In other hand soil exhibits an equivalent Poisson's ratio almost equal to 0.5. (Britto & Gunn, 1987)

The undrained capability of the implemented subroutine would be applied to ice gouging problem in future.

## 6 ACKNOWLEDGEMENTS

The first author gratefully acknowledges funding from the PIRAM JIP and C-CORE.

## 7 REFERENCES

- Barrette, J., & Phillips, R. (2011). Ice Keel-Seabed Interaction: Numerical Modelling for Sands. *Conference on Ports and Ocean Engineering Under Arctic Conditions (POAC)*.
- Been, K., & Jefferies, M. G. (1985). A state parameter for sands. *Geotechnique*, 35(2), 99-112.
- Bishop, A. W. (1966). The strength of soils as engineering materials. *Geotechnique*, 16(2), 89-13.
- Bolton, M. D. (1986). The strength and dilatancy of sands. *Geotechnique*, 36(1), 65-78.
- Britto, A. M., & Gunn, M. J. (1987). *Critical State Soil Mechanics via Finite Elements*. Ellis Horwood Limited.
- Cubrinovski, M., & Ishihara, K. (1998). Modelling of sand behaviour based on state concept. *Soils and Foundations*, 38(2), 115-127.
- Eskandari, F., Phillips, R., & Hawlader, B. (2010). A State Parameter Modified Drucker-Prager Cap Model. *Canadian Geotechnical Conference*.
- Gajo, & Wood, D. M. (1999). Seven-Trent sand, a kinematic hardening constitutive model: the q-p formulation. *Geotechnique*, 49, 595-614.
- Ishihara, K. (1993). Liquefaction and flow failure during earthquakes. *Géotechnique*, 43(3), 351-415.
- Jefferies, M. G., & Been, K. (2006). *Soil Liquefaction*. Taylor & Francis.
- Jefferies, M. G., & Shuttle, D. A. (2002). Dilatancy in general Cambridge-type models. *Géotechnique*, 52(9), 625-638.
- Jefferies, M. G., & Shuttle, D. A. (2005). Norsand, features, calibration, and use. *Soil constitutive models: evaluation, selection and calibration*. Edited by J. A. Yamamuro and V. N. Kaliakin. ASCE Geotechnical Special Publication 128, 204-236.
- Kenny, S., Phillips, R., Clark, J., & Nobahar, A. (2005). PRISE numerical studies on subgouge deformations and pipeline/soil interaction analysis. *Proceedings of the 18th Conference on Ports and Ocean Engineering Under Arctic Conditions (POAC)*, 1, pp. 43-52. Potsdam, NY, USA.
- Li, X. S., Dafalias, Y. F., & Wang, Z. L. (1999). State dependent Dilatancy in critical state constitutive modeling of sand. *Can Geot. J.*, 36, 599-611.
- Manzari, M., & Dafalias, Y. F. (1997). A critical state two-surface plasticity model for sands. *Geotechnique*, 47, 255-272.
- Roscoe, K. H., & Poorooshasb, H. B. (1963). A fundamental principle of similarity in model tests for earth pressure problems. *2nd Asian Conference on Soil Mechanics*, (pp. 134-140).
- Verdugo, R. (1992). *Characterization of sandy soil behavior under large deformation*. Ph.D. thesis, University of Tokyo, Tokyo, Japan.
- Wan, R. G., & Guo, P. J. (1998). A simple constitutive model for granular soils: modified stress-dilatancy approach. *Computers and Geotechnics*, 22, 109-133.